Proceedings of the 8th International Conference on MicroManufacturing
University of Victoria, Victoria, BC, Canada, March 25-28, 2013

Electrochemical Polishing of Microcomponents

ICOMM
2013
No.

D. Berestovskyi[1], M.P. Soriaga[2], P. Lomeli[3], J. James[4], B. Sessions[5], H. Xiao[6], W.N.P. Hung[7]
[1]Mechanical Engineering Dept., Texas A&M University, USA; d.berestovskiy@gmail.com
[2]Chemistry Dept., Texas A&M University, USA; soriaga@mail.chem.tamu.edu
[3]Santa Rosa Div., Agilent Technologies, USA; paul_lomeli@agilent.com
[4]Santa Rosa Div., Agilent Technologies, USA; jon_james@agilent.com
[5]Chemistry Dept., Texas A&M University, USA; bjsessions@tamu.edu
[6]Chemistry Dept., Texas A&M University, USA; hxiao@tamu.edu
[7]Engineering Technology Dept., Texas A&M University, USA; hung@tamu.edu

Key Words: electrochemical, polishing, micromachining, deburring

ABSTRACT

Microcomponents can be fabricated by traditional methods like micromilling/drilling, or by nontraditional methods like electrical discharge micromachining (EDM), laser micromachining, or electrochemical micromachining (ECM). These methods, however, often leave detrimental residual defects like sharp burrs, cracks in heat affected zones, in addition to rough surface finish. Electrochemical polishing (ECP) offers a non-contact technique to remove surface defects such as burrs, rolling/grinding/machining marks regardless of component size. This study develops an ECM/ECP technique to fabricate or polish microcomponents, and implements this technique to polish copper, titanium, and stainless steel microcomponents fabricated by EDM and micromilling. Assessment is made by optical microscopy, electron microscopy, atomic force microscopy, and interferometry. Burrs and surface defects of the tested microcomponents are effectively removed by ECP. Surface finish of polished surfaces of polycrystalline titanium, copper, and stainless steels is in the range of 100-300 nm R_a on polycrystalline surface and 1-10 nm R_a within a single grain.

A. INTRODUCTION

Material removal techniques have a pivotal role to play in component fabrication. Many high strength alloys such as copper beryllium, titanium, cobalt, stainless steel, and NiTi shape memory alloys were required for microdevices but they are difficult to machine using the traditional processes due to induced subsurface damage of the workpiece, excessive burrs, and short tool life. Laser and electrical discharge machining (EDM) can produce microfeatures but with compromised quality. Electrochemical micromachining (ECM) is among key technologies for semiconductor, electro communication, optics, medicine, bio technology, automotive, avionics, and ultraprecision machinery industries. ECM technique has replaced the chemical etching process which was predominantly being used in these industries because of the many advantages it offered [1, 2]. Microfabrication by ECM can be done through mask or maskless techniques [1]. The latter requires a better degree of tooling and process control compared to the conventional ECM technique. The selection of electrolyte is very critical because of the extremely small gap between the tool and the workpiece. Though ECM has a lot of scope for micromachining, there are a number of technical issues that need to be addressed such as stray material removal, tool structure, and machining gap [1].

Surface finishing can also be controlled by ECM because it removes material at the microlevel. This technique was employed in the manufacturing of micronozzles [1]. When appropriate parameters and suitable electrolyte are utilized the same process becomes electrochemical polishing (ECP) to either deburr, polish previously machined microfeatures, or to reveal grain structures for metallographic study [3].

The objectives of this research are to:

(i) Develop an ECM/ECP technique with closed loop control, and
(ii) Apply the technique to polish and remove burrs on microcomponents.

B. EXPERIMENT

Microcomponents of copper alloy, stainless steel, and titanium were fabricated by different techniques and polished by ECP.

- Copper. Microcomponents on a beryllium copper alloy sheet (CA173, 100μm thick) were cut by wire-type electrical discharge machining (EDM). The microcomponents were cleaned in diluted H_2SO_4 for 15 minutes at 55°C to remove any possible contamination after EDM, and then polished by ECP. Two types of electrolytes were tested: the first electrolyte was sodium based, while the second type was a mixture of sodium electrolyte with addition of H_2SO_4 till pH=2. All tests were performed at 50 KHz, 32 mA/mm^2 current density. The cathodic electrode (316L stainless steel, Ø1.34 mm) was programmed to travel at 0.35 mm/s and 1.5 mm above and along a row of microcomponents. A polished 316L stainless steel

cathode with ϕ500 µm diameter was used. A column of fresh sodium based electrolyte that housed the cathode hovered above the anode with a 3-degree-of-freedom computer controlled manipulator to maintain a constant gap of 50-200 µm between anode and cathode. All copper microcomponents were cleaned in water, dried, and stored in a desiccator.

- Stainless steels. Both 304 and 316L stainless steel sheets of 0.5-1 mm thick were wire EDM cut to smaller samples. Microchannels were micromilled on some samples with ϕ152-192 µm milling tools in minimum quantity lubrication (MQL). Acidic and alcohol based electrolytes were developed for stainless steels alloys. Other polycrystalline 304 stainless steel plates were fabricated, coated with a photoresist, and etched to form a pattern. A resist layer was 4-5 µm thick with different patterns; slots of 126 µm width were chosen for the study. Both solid (Ø728 µm) and hollow (Ø523 µm OD, Ø193 µm ID) stainless steel electrodes were used. The electrodes were positioned in either vertical or horizontal flow positions.
- Titanium. The commercially pure titanium samples were prepared similarly to stainless steel sheets. Thin titanium sheets of 0.5-1 mm thick were wire EDM cut, and then either polished or micromilled then polished. Acidic and alcohol based electrolytes were developed for titanium .

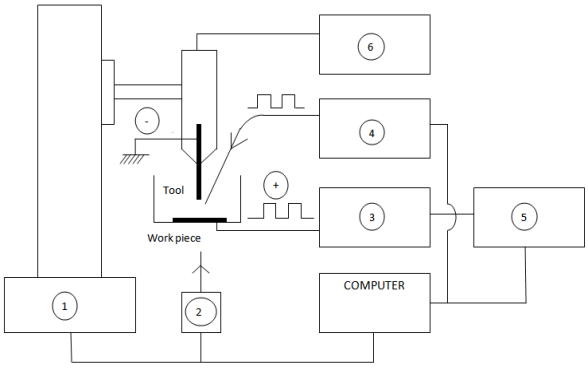

Fig. 1: Schematic of experimental setup. The integrated and computer-controlled system includes (1) Velmex VXM-1, 5-axis positioner, (2) Keyence LKG 87 laser sensor, (3) Agilent 33250A function generator and Agilent 33502A amplifier, (4) IPG YLR 200 fiberlaser, (5) Tektronix TDS 1002B digital oscilloscope, and (6) electrolyte pump.

A customized ECM/ECP cell was built (Fig. 1). Power was either provided with an Agilent function generator 33250A and Agilent amplifier 33502A for square voltage pulses of 16-24 Vpp at 50Hz-1MHz range or with a DC Galvanostat. Both open-loop and closed-loop control schemes were implemented to maintain the gap based on current feedback. Microcomponents were examined with a measuring Olympus STM7 microscope, JEOL JSM-400 scanning electron with an integrated energy dispersive X-ray spectroscopy (EDS) system, or Digital Instrument atomic force microscope. Surface finish was measured with a Zygo interferometer.

C. RESULT

Consider a string of burr along the edge of an EDM surface, a burr is modeled as an absolute sine wave. The total volume of burr can be shown to be [4]:

$$V_L = \frac{bL}{D}\frac{\pi h^2}{2}\int_0^{P/2} sin^2\left(\frac{2\pi x}{P}\right) dx \quad (1)$$

Where
V_L : burr volume along a length L
b : number of burrs under the tool
D : electrode diameter
h : maximum burr height
P : burr period

The ECM/ECP process removes a volume of material in a single pulse according to Faraday's and Ohm's laws:

$$V_u = \int_0^{\tau} \frac{CEAdt}{gr} \quad (2)$$

$$C = \frac{100}{F\sum_i\left(\frac{x_i z_i}{A_i}\right)\frac{100}{\sum_i\left(\frac{x_i}{\rho_i}\right)}} \quad (3)$$

Where
E : voltage
A : electrode area
A_i : atomic weight of element i
t : time
g : interelectrode gap
r : electrolyte resistivity
x_i : element percentage
ρ_i : density of element i
τ : pulse on-time

Material removal rate (MRR) for each pulse is simply:

$$MRR = \frac{V_u}{\tau} \quad (4)$$

Polishing time can be estimated by calculating the number of pulses and pulse frequency. The number of pulses to remove burrs along a distance L is:

$$N = \frac{V_L}{V_u} \quad (5)$$

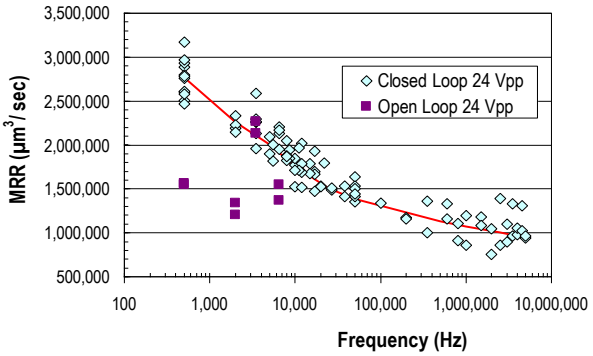

Fig. 2: Open-loop and closed-loop material removal rate as a function of pulse frequency. 316L stainless steel, ϕ0.5 mm electrode, sodium based electrolyte, 16-24 Vpp.

Consistent *MRR* is obtained with closed loop control system using current density as feedback signal to adjust the electrode gap [5]. As predicted by equations (3, 4), the *MRR* increases with applying voltage, but decreases with shorter pulse duration or higher pulse frequency (Fig. 2).

Deburring is necessary to remove material residues after a manufacturing process. Manual deburring is tedious, time consuming, and prone to human error. Chemical etching removes burr but also compromise geometry of a microcomponent. As expected, the EDM process produces significant recast layer (burr) of copper and oxide along the edges of the microparts (Fig. 3a). After cleaning any oxidized layer chemically, the remaining rough surface is successfully deburred and polished by ECP process at high frequency (Fig. 3b). The sodium based electrolyte, however, removes material preferentially and reveals grain boundaries of the polished CA173 alloys. This is not an issue for the microcomponents under this study since they are used in microelectronic applications. For an application when high dynamic stress is expected, then grain boundary depletion would be a concern. Back scattered electron imaging and X-ray dot mapping shows a loop is completely cleared of burrs and other EDM by-products. Back scattered electron imaging and X-ray dot mapping shows a loop is completely cleared of burrs and other EDM by-products (Figs. 4a and 4b).

The ECM technique can be used to remove material under a patterned mask. Figure 5 shows a stainless steel sample before and after ECM. The process, however, causes undercut underneath a mask, and rounded corners of sharp pattern. When a fast removal rate is obtained with high current, the surface finish is compromised (Fig. 5b) and required subsequent polishing.

Being a noble material, titanium is extremely stable due to its oxide layer on the surface. Although a solution of sodium bromide and sodium nitrate can be used effectively removes the oxide and titanium by µECM, the resulted rough surface requires another polishing step by ECP.

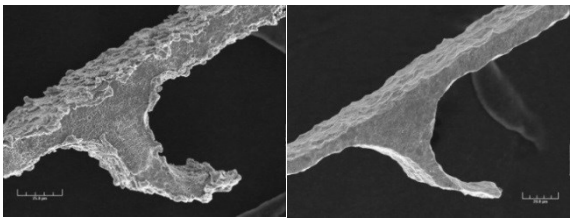

(a) ***(b)***

Fig. 3: (a) Microcomponent after EDM, and (b) after polished by ECP. CA173, ϕ0.5 mm electrode, 50 KHz, sodium based electrolyte.

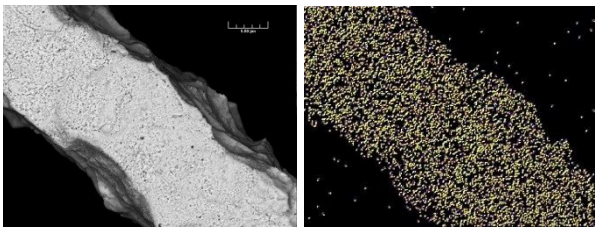

(a) ***(b)***

Fig. 4: (a) Back scattered electron image of a copper microcomponent after µECM, and (b)Copper X-ray mapping of the same loop showing a clean copper substrate.

(a) ***(b)***

Fig. 5: ECM sample (a) with pattern resist before ECM, and (b) pattern after ECM and with resist removed. 304 stainless steel, sodium based electrolyte, 0.5 mm gap, 1 kHz, 380 mA.

Microdrilling and micromilling are effective techniques to remove materials by conventional methods. Excessive burrs and surface defects due to micromachining present an opportunity for ECP. Figure 6a shows the closed up of a cross channel produced by micromilling. Burrs at top of the channels, and at crossing junction, tool feed marks, and grooving lines parallel to the channel due to missing grains of a microcutting tool are seen. These defects are effectively removed after ECP (Figs. 6b, 9, 10). The surface finish of 304 stainless steel samples is somewhat deteriorated due to the presence of impurities in grain boundaries. With proper metallurgical refinement, there are less impurities in the implanted grade 316L stainless steel.

This results in smoother surface of a polished 316L as compared to that of 304 stainless steel. Surface finish measurement by white-light interferometry shows a surface finish range of 100-300 nm R_a at both the plate and bottom of the channels.

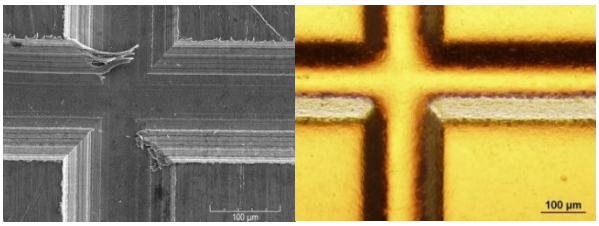

(a) *(b)*

Fig. 6: (a) Microchannel after micromilling, and (b) after polished by ECP. 304 stainless steel, H_3PO_4 solution, 2.5A/cm^2, 400s.

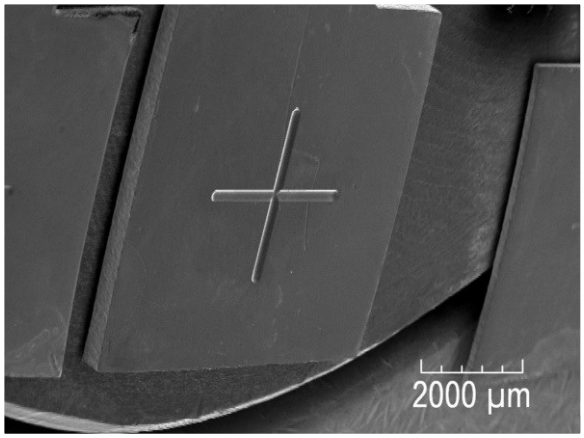

Fig. 7: Milling of microchannel on stainless steel, and titanium.

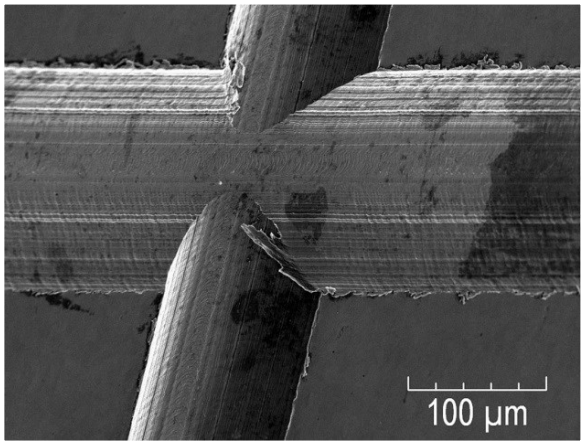

Fig. 8: Closed up of milled microchannels on 316L stainless steel. Notice the excessive burrs at the cross junction.

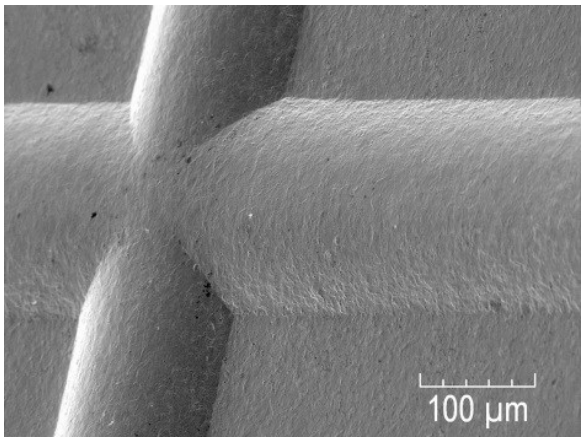

Fig. 9: The milled cross junction of 304 stainless steel after ECP.

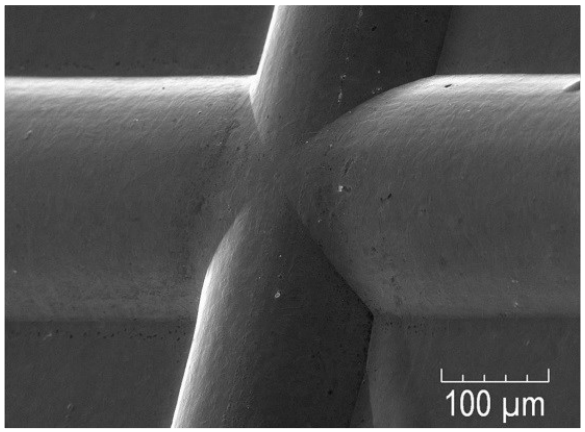

Fig. 10: The milled cross junction of 316L stainless steel after ECP.

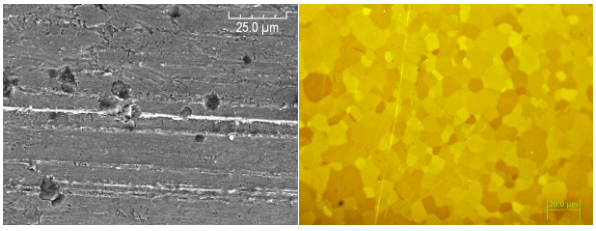

(a) *(b)*

Fig. 11: (a) Scanning electron image of as-received titanium sheet. There are numerous defects due to rolling operation. (b) Optical image of polished titanium. The grains are enhanced by polarized light. ECP in alcohol based after 20 minutes.

Atomic force microscopy examination shows rough surface of titanium samples after ECM (Fig. 12) and smooth surface of the same sample after ECP (Figs. 13 and 14). As expected, the root-mean-square surface finish (340 nm after ECM) is drastically reduced to 42nm after ECP (Fig. 13). When measuring within a grain boundary, the area surface finish is 1-10 nm (Fig. 14).

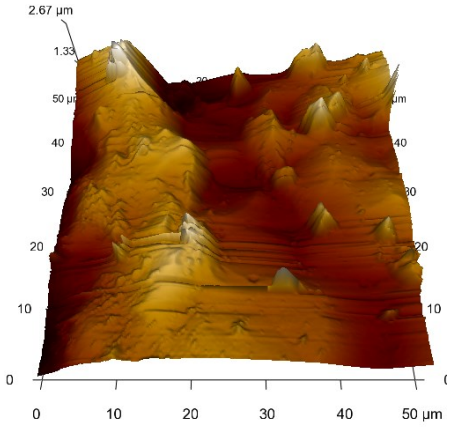

Fig. 12: Atomic force microscopic image of titanium after ECM for 90 second in potassium and sodium electrolyte solution. Surface finish 340 nm R_{rms}.

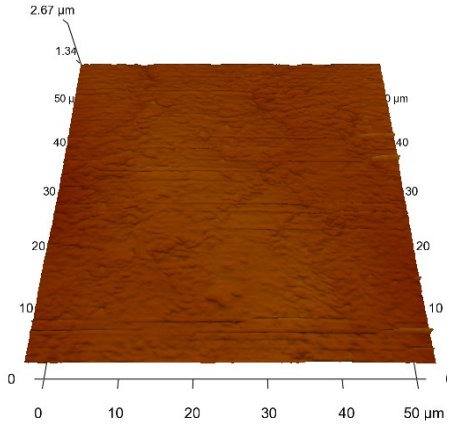

Fig. 13: Atomic force microscopic image of titanium after ECP for 20 minutes in alcohol based electrolyte. Surface finish 42 nm R_{rms}.

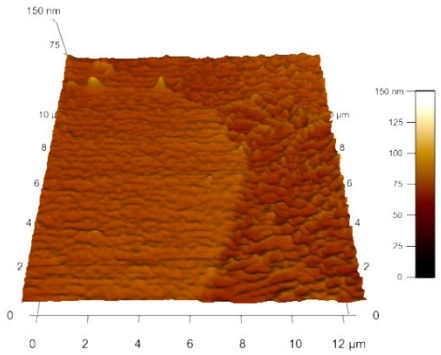

Fig. 14: Atomic force microscopic image of two adjacent titanium grains after ECP for 20 minutes in alcohol based electrolyte. Notice the change across the grain boundaries. Surface finish 1-10 nm R_{rms} within a grain.

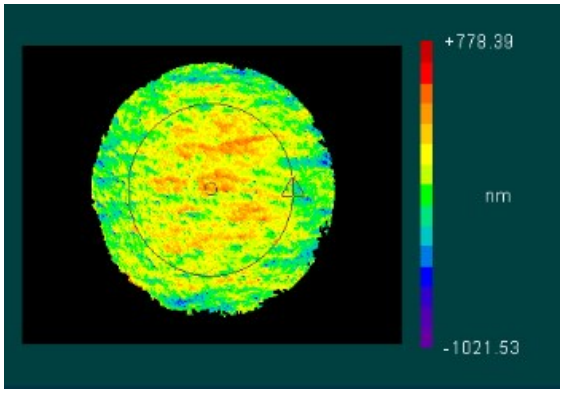

Fig. 15: Surface profile of 304 stainless steel after ECP in laminar flow condition. ECP in acid based electrolyte, 400s.

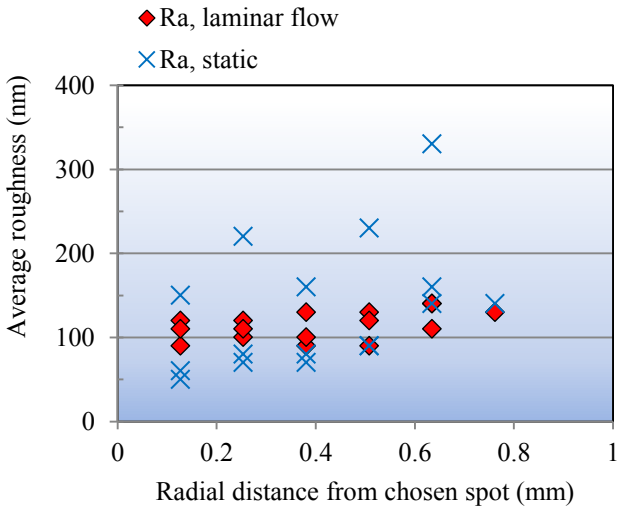

Fig. 16: Effect of electrolyte flow on surface finish. ECP 304 stainless steel after 400 in alcohol based electrolyte.

How electrolyte flows between electrodes affects the quality of polished surface. By adjusting the pump to get static to uniform laminar flow, surface finish of the 304 stainless steel samples varies Figure 15 shows typical profile of ECP sample after interferometry measurement. By varying the radial distance and computing surface roughness along a circular cut, surface roughness of an entire surface can be characterized. Much variations are found for surface submerged in static electrolyte, and the opposite is true for laminar flow case. Although surface roughness at several spots on a polished samples were compatible to that after polishing in the laminar flow condition, the range of surface roughness after static electrolyte polishing is much higher (Fig. 16).

D. SUMMARY

Electrochemical micromachining and electrochemical micro/nano polishing are developed. When applying to copper, stainless steel, and titanium, the study shows:

1) Closed loop current feedback at high frequency provides a more consisting material removal rate.
2) Burrs and other surface defects produced by EDM or micromilling are effectively removed by ECP.
3) Surface finish value of typical polished grain is 1-10 nm R_a, but that from polished polycrystalline grains is 100-300 nm R_a.
4) A laminar flow of electrolyte produces more uniform surface finish.

REFERENCES

[1] K.P. Rajurkar et al., "Micro and Nano Machining by Electro-Physical and Chemical Processes." *Annals of the CIRP*, 2006; 55:2, 643-666.

[2] H. Hocheng et al., "A Material Removal Analysis of Electrochemical Machining Using Flat-End Cathode." *Journal of Materials Processing Technology*, 2003; 140:1-3, 264-268.

[3] J. Geough, *http://www.electrochem.cwru.edu/ed/encycl/*. Access date 05/25/2007.

[4] S.S. Sundarram, "Development of Electrochemical Micromachining," Thesis, Texas A&M University, 2008.

[5] F.M. Ozkeskin, "Feedback Controlled High Frequency Electrochemical Micromachining," Thesis, Texas A&M University, 2008.